ingegneria sismica
International Journal of Earthquake Engineering
Anno XLIII - Num. 1 - 2026

Autonomous scheduling method for hybrid demand response in microgrid of industrial park under multi-agent cooperation framework

Fuchun Deng[1,*]

[1] School of Big Data Technology, Chongqing College of Finance and Economics, Yongchuan 402160, ChongQing, China

SUMMARY: *Under the background of the "double carbon" goal promotion and the energy system reconstruction of industrial parks, facing the intertwined problems of new energy fluctuations, load time-varying and user response uncertainty, this paper proposes an autonomous scheduling method for hybrid demand response of industrial park microgrid under the framework of multi-agent cooperation. Based on the three-layer architecture of data perception, resource coordination and coordination decision, the model integrates dynamic trapezoid-shaped fuzzy modeling of interruptable load, spatio-temporal and behavioral coupling prediction of electric vehicles, day-ahead economic scheduling and intra-day rolling robust correction, and introduces a three-level response mechanism of core-elasticity-emergency. The experimental results show that the average load modeling error of the model is 6.9%, the hot spot matching rate of electric vehicles is 90.0%, the Accuracy and F1 are 93.7% and 92.5%, respectively. Under the four typical scenarios, the average regulation cost is reduced by 24.3% compared with the traditional strategy, the average renewable energy consumption rate reaches 80.3%, and the average power recovery time is shortened to 32 minutes. The research results show that this method is of great significance to improve the economy, flexibility and stability of the park microgrid.*

KEYWORDS: *Multi-agent cooperation; Industrial park microgrid; Hybrid demand response; Autonomous scheduling*

1 Introduction

Under the background of the continuous promotion of the "double carbon" goal and the accelerated reconstruction of the park energy system, the industrial park microgrid has become an important carrier to undertake the collaborative operation of distributed photovoltaic, wind power, energy storage and flexible load. At the same time, the volatility of renewable energy output, the strong time-varying industrial production load, and the uncertainty of user-side response behavior add up to each other, which makes the park operation face more prominent risk of supply-demand imbalance. Project materials show that in 2024, the average power abandonment rate of renewable energy in industrial parks in China is still at a high level, and the response of existing scheduling technologies to multi-scale disturbances under a high proportion of new energy access is still insufficient, which is easy to cause problems such as power deviation amplification, storage regulation mismatch, and local energy supply stability decline. This indicates that we still need to further improve the collaborative response ability to multi-source disturbances and dynamic fluctuations when carrying out the research on

*dfccqcj@yeah.net
https://doi.org/10.65102/is2026216
Published: 30 April, 2026

microgrid scheduling for complex park scenarios.

Demand response is considered to be the key to improve the flexibility of campus microgrid, but there are still obvious shortcomings in the actual modeling of existing research. One kind of methods pay more attention to the optimization of the source side and the energy storage side, and treat the demand-side resources as simple constraints, which is difficult to reflect the dynamic changes of user behavior in industrial scenarios affected by temperature, electricity price, production rhythm and subjective preferences. Although the other kind of methods introduce flexible resources such as electric vehicles and interrusible loads, they often use static probability or fixed threshold to describe the response characteristics, which is insufficient to reveal the nonlinear coupling relationship in complex scenarios, especially difficult to deal with the problem of continuous regulation and hierarchical response under multi-source uncertainty. The project book also pointed out that there were still common bottlenecks in current research, such as insufficient description of user bounded rationality characteristics and secondary imbalance easily caused by single-stage trigger mechanism. From this point of view, it is necessary to further integrate demand-side behavior differences, response level switching and real-time scheduling process.

Based on this, this paper focuses on the autonomous scheduling problem of hybrid demand response in microgrid of industrial parks, and constructs a scheduling model for multi-agent interaction in the framework of multi-agent cooperation. The research is carried out from three aspects. Firstly, according to the characteristics of the interruffable load response boundary changing dynamically with the environment and price, the dynamic trapezoidal fuzzy modeling and adaptive membership mechanism are introduced to enhance the ability to characterize the time-varying load. Secondly, for the temporal and spatial migration and behavioral differences of EV charging demand, Gaussian mixture model (GMM), non-homogeneous Markov chain (NMN) and state-dependent electricity price response mechanism are integrated to describe the coupling relationship among travel chain, state of charge (SOC) and charging decision. Thirdly, a two-stage optimization framework of "day-ahead economic dispatching-intra-day robust correction" is constructed around the smoothing of power fluctuations and the coordination of operation economy, and the adaptive scheduling in multiple scenarios is realized through the three-level response mechanism of "core-elastic-emergency".

In this paper, we hope to solve not only a scheduling problem in the traditional sense, but also attempt to truly connect the demand-side behavior analysis, hybrid uncertainty quantification and multi-time scale optimization, so as to make the scheduling process of industrial park microgrid change from one-way control to autonomous decision-making under multi-agent collaboration. Through this research, we hope to not only improve the level of renewable energy consumption and shorten the recovery time of power deviation, but also provide method support for the industrial park to build a more flexible and intelligent energy operation mode.

2 Literature Review

Focusing on the optimal scheduling problem of microgrid in industrial parks, the existing research has carried out many explorations from the perspectives of capacity allocation, operation control, demand response and intelligent optimization. According to relevant reports released by China Energy Research Society, under the background of continuous improvement of new energy penetration, the energy system of industrial parks is still facing realistic pressures such as high power abandonment rate, enhanced load fluctuation and local supply-demand imbalance [1]. In terms of sources-storage collaboration, Li et al. proposed a bilevel optimization based optical storage capacity allocation method, which provides a reference for

microgrid planning and operation collaboration [2]. For multi-energy micro-grid scenarios in smart parks, Situ et al. used typical scenario sets to carry out multi-objective configuration optimization, which enhanced the overall ability of economy and reliability under complex conditions [3]. El Mezdi et al. integrated renewable energy, electric vehicles and multi-source microgrid control into the energy management framework, indicating that multi-resource collaboration has become an important direction of current microgrid research [4]. However, most of these researches still focus on the coordination optimization of source-network storage side, and the description of demand-side behavior differences and their uncertainties is not sufficient.

With the deepening of the concept of source-load interaction, demand response has gradually become an important part of microgrid dispatching research. Wang et al. systematically sorted out the application methods and development trends of demand response from the perspective of resource potential assessment, and pointed out that flexible load has strong adjustment potential [5]. On this basis, Kong et al. proposed a multi-time node response potential evaluation method of adjustable resource cluster considering the influence of dynamic process, which improved the timing of response ability analysis [6]. Fan et al. discussed the demand response mechanism in the context of the new power system, emphasizing the synergistic relationship between price signals, incentives and system regulation objectives [7]. Furthermore, Li et al. incorporated multiple demand response and electric vehicles into the day-ahead stochastic optimization scheduling model of microgrid, which expanded the depth of demand-side resources participating in scheduling decision-making [8]. However, from the existing research, many models still use static parameters or average response methods to describe user behavior, which is difficult to accurately reflect the dynamic change characteristics of interruptable load in industrial parks under the influence of temperature, electricity price, production rhythm and user psychology.

In addition to demand response, energy storage collaboration, market mechanism and intelligent algorithm also provide new ideas for microgrid scheduling research. Zhu et al. proposed a hybrid energy storage coordination optimization strategy based on hierarchical control, indicating that hierarchical cooperation is conducive to improving system operation resilience [9]. Starting from the multi-micro-grid distribution system, Zhao et al. Studied the interval scheduling method and market trading strategy, and expanded the scheduling analysis perspective in the multi-agent game scenario [10]. Ji et al. introduced deep reinforcement learning into online optimal scheduling of microgrid, making the scheduling method show a trend of evolution from rule driven to data driven [11]. However, there are still two shortcomings in the existing methods in the application of industrial parks. On the one hand, the fuzziness, randomness and behavior coupling characteristics in hybrid demand response are not deeply mined. On the other hand, most studies are still focused on single-stage or single-layer optimization, and the connection between day-ahead decision-making and intra-day correction, multi-level response triggering and multi-agent cooperation mechanism are insufficiently considered.

In general, the existing researches provide a rich theoretical basis and methodological support for microgrid scheduling in industrial parks, but there is still room for further expansion in the dynamic fuzzy representation of interrable load, the spatiotemporal behavior modeling of electric vehicle charging, and the two-stage collaborative optimization driven by hybrid demand response. Therefore, under the framework of multi-agent collaboration, this paper proposes to integrate the dynamic fuzzy modeling of interrusible load, the spatio-temporal behavior coupling analysis of electric vehicles, and the autonomous scheduling mechanism of "day-ahead economic dispatching-intra-day robust correction", so as to improve the flexible adjustment ability and stable operation level of the microgrid in industrial parks in high

fluctuation scenarios.

3 Construction of autonomous scheduling model for hybrid demand response in microgrid of industrial park under the framework of multi-agent cooperation

3.1 Design of multi-agent cooperative scheduling architecture in microgrid of industrial park

Industrial park microgrid has the characteristics of multiple distributed power access, complex load structure, strong heterogeneity of demand response subjects and high coupling degree of operation constraints. If the single-center and static threshold scheduling method is still adopted, it is often difficult to timely deal with the disturbance caused by the joint superposition of wind power fluctuation, interrable load response deviation and electric vehicle charging demand migration. Aiming at the coexistence of multi-source information coupling, time-varying load response boundary, dynamic migration of electric vehicle charging behavior and hierarchical regulation requirements in the microgrid of industrial parks, this paper builds a multi-agent cooperative scheduling architecture composed of data perception layer, resource coordination layer and coordination decision layer. In order to form a closed loop operation chain connected with state perception, local response, global coordination and feedback correction.Figure 1 shows the multi-agent cooperative scheduling architecture of microgrid in industrial park.

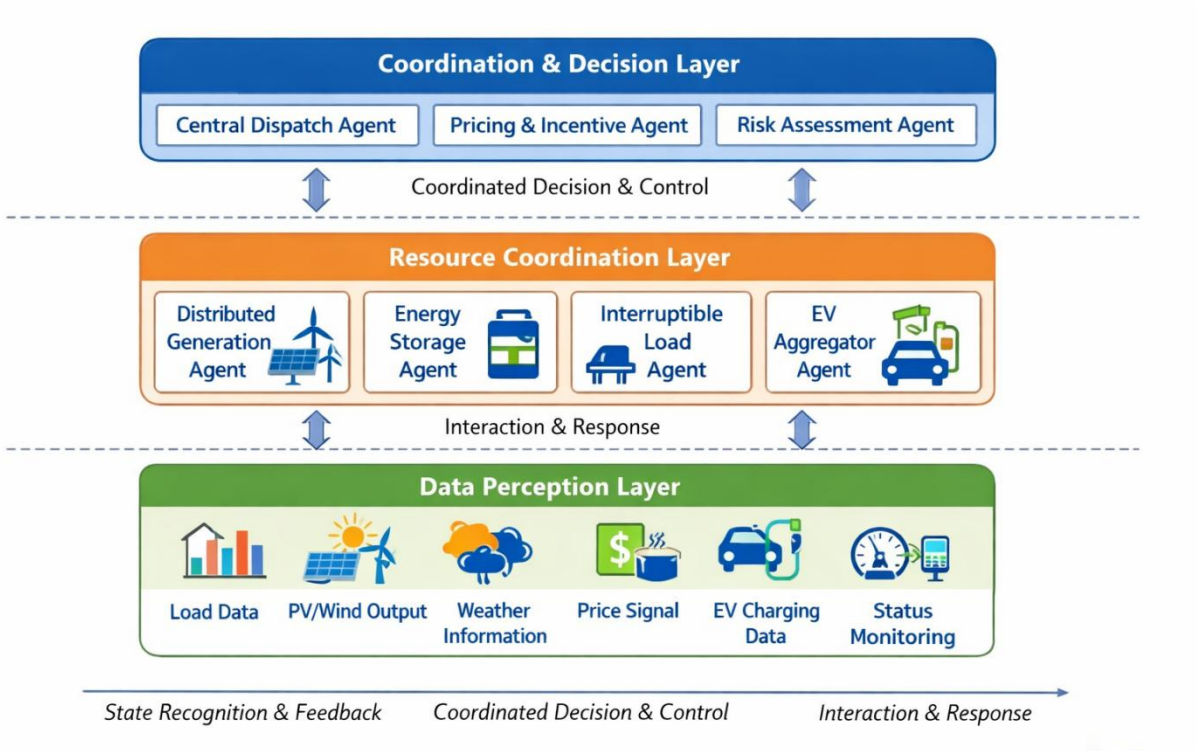

Figure 1: Autonomous scheduling architecture of industrial park microgrid with multi-agent cooperation

The bottom layer of the figure is responsible for collecting load data, landscape output, meteorological information, electricity price signals, charging records of electric vehicles and equipment status. The middle layer was composed of distributed power agent, energy storage

agent, interrable load agent and electric vehicle aggregation agent, which was responsible for local state analysis and flexible response execution. In the upper layer, a central scheduling agent, a price incentive agent and a risk assessment agent are set up to coordinate the consistency of various local decisions and correct the security constraints.

(1) State aggregation design of data-aware layer

The data-aware layer is the input of the whole scheduling architecture, and its core task is to convert the operation information under heterogeneous, scattered and different time scales into a unified state that can be called by each agent. Let the system state vector at time t be as follows.

$$S_t = \left[P_t^{pv}, P_t^{wt}, L_t^b, L_t^{il}, L_t^{ev}, SOC_t, \lambda_t, W_t\right]^T \tag{1}$$

where, P_t^{pv} and P_t^{wt} represent the output of photovoltaic and wind power respectively, L_t^b is the base load, L_t^{il} is the interchangeable load, L_t^{ev} is the charging demand of electric vehicles, SOC_t is the state of charge of energy storage, λ_t is the real-time electricity price, W_t is the meteorological disturbance factor. Through this state representation, the key variables highlighted in the project book, such as temperature, electricity price, load and EV behavior, can be uniformly incorporated into the same information interface to provide standardized inputs for subsequent collaborative decision making.

(2) The design of autonomous agent in resource coordination layer

The resource collaboration layer is the core of the multi-agent architecture. The distributed power agent is responsible for identifying the fluctuation trend of new energy output, and feedback the adjustable output interval to the upper layer. The energy storage agent switches charge and discharge according to SOCt and power shortage. The interruptible load agent evaluates the load reduction space according to the comprehensive changes of temperature, electricity price and user production plan. The aggregation agent of electric vehicles computes the group charging and discharging tendency by combining charging hotspot migration, travel chain state and dynamic electricity price. To describe the autonomous decision output of the local agent, let the action of the type i resource agent at time t be as follows.

$$a_i(t) = \pi_i(s_i(t)) \tag{2}$$

Here, $s_i(t)$ is the local observed state of agent i and $\pi_i(\cdot)$ is the corresponding decision map. Therefore, each agent can not only retain its own physical constraints and behavior differences, but also access the upper coordination module through a unified interface, so as to avoid the solution pressure and response delay caused by a single master directly processing all fine-grained information.Table 1 shows the function division and main interaction information of various agents.

Table 1: Multi-agent function division and main interaction information

Agent Name	Core Responsibility	Main Inputs	Main Outputs	Coordinated With
Central Dispatch Agent	Aggregates local decisions and generates global dispatch commands	System states, candidate actions from each agent	Global power allocation scheme	All resource agents
Price Incentive Agent	Generates time-of-use prices and compensation signals	Load level, market electricity price, response gap	Price incentive parameters	Interruptible Load Agent, EV Aggregation Agent
Risk Assessment Agent	Identifies power imbalance and limit-violation risks	Output forecast errors, energy storage states, disturbance information	Risk level, triggering thresholds	Central Dispatch Agent
Distributed Generation Agent	Evaluates available wind/PV output and fluctuation boundaries	Meteorological information, equipment states	Adjustable output interval	Central Dispatch Agent, Energy Storage Agent
Energy Storage Agent	Executes charging/discharging and reserve support	Power deficit, SOC	Charging/discharging power	Central Dispatch Agent
Interruptible Load Agent	Estimates load shedding potential and response intensity	Temperature, electricity price, production tasks	Load reduction power, response willingness	Price Incentive Agent
EV Aggregation Agent	Aggregates charging/discharging demand and adjusts spatiotemporal distribution	Trajectory information, charging records, electricity price	Charging transfer amount, V2G power	Central Dispatch Agent, Price Incentive Agent

(3) The consensus control design of the coordination decision layer

The coordination decision layer does not replace the local agent, but is responsible for completing the global consistency correction under the multi-objective constraints. Considering that the core goals of the microgrid in industrial parks are to weaken power deviation, reduce regulation costs and improve the absorption capacity of renewable energy, the following coordination objective function can be constructed:

$$\min F = \omega_1 C_t + \omega_2 \Delta P_t + \omega_3 R_t \tag{3}$$

Here, C_t represents the integrated operating cost, ΔP_t represents the power deviation of the source charge, Rt represents the risk penalty term, and ω_1,ω_2,ω_3 are the weight coefficients. At the same time, the system should meet the power balance relationship:

$$P_t^{pv} + P_t^{wt} + P_t^{es} + P_t^{grid} + P_t^{dr} = L_t^b + L_t^e \tag{4}$$

where, $P_t^{es}$is the regulated power of energy storage, P_t^{grid} is the power exchanged with the superior grid, and P_t^{dr} is the equivalent regulated power formed by demand response. The expression unifies the regulation results of source, storage, load and vehicle into the same power balance framework, and also provides a structural basis for the subsequent two-stage optimization and three-stage response triggering.

(4) Design of architecture closed-loop and hierarchical response interface

Considering that there are both normal fluctuations and sudden disturbances such as high temperature shocks, sudden price changes and centralized charging in the microgrid operation of industrial parks, this paper reserves a hierarchical response interface at the architecture layer. According to the real-time deviation and the scene intensity, the risk assessment agent identifies whether it enters the core level, elastic level or emergency level response interval, and sends the threshold information back to the central scheduling agent and the price incentive agent, so that the local agents can switch different control modes under different disturbance intensity. The multi-agent cooperative scheduling architecture can not only complete multi-source data access and local autonomous control, but also be compatible with the dynamic fuzzy modeling of interruptable load downward and the two-stage autonomous scheduling method of "day-ahead economic dispatching and intra-day robust correction" upward, which makes the model have better hierarchy and scalability.

3.2 Design of two-stage autonomous scheduling method driven by hybrid demand response

The power imbalance in the microgrid of industrial parks is closely related to the change in the intensity of interrable load response, the migration of electric vehicle charging behavior, and the price signal transduction bias. If only single-stage static scheduling method is used, it is often difficult to balance the economy of day-ahead planning and the timeliness of intra-day correction. To this end, we construct a two-stage autonomous scheduling method driven by hybrid demand response, in which the results of dynamic fuzzy modeling of interruptable load and the spatio-temporal behavior prediction of electric vehicle charging are embedded into the scheduling process together, and multi-time scale collaboration is realized through a chain mechanism of "day-ahead optimization generation benchmark, intra-day rolling correction deviation, and hierarchical response fast execution". The two-phase autonomous scheduling process driven by hybrid demand response is shown in Figure 2.

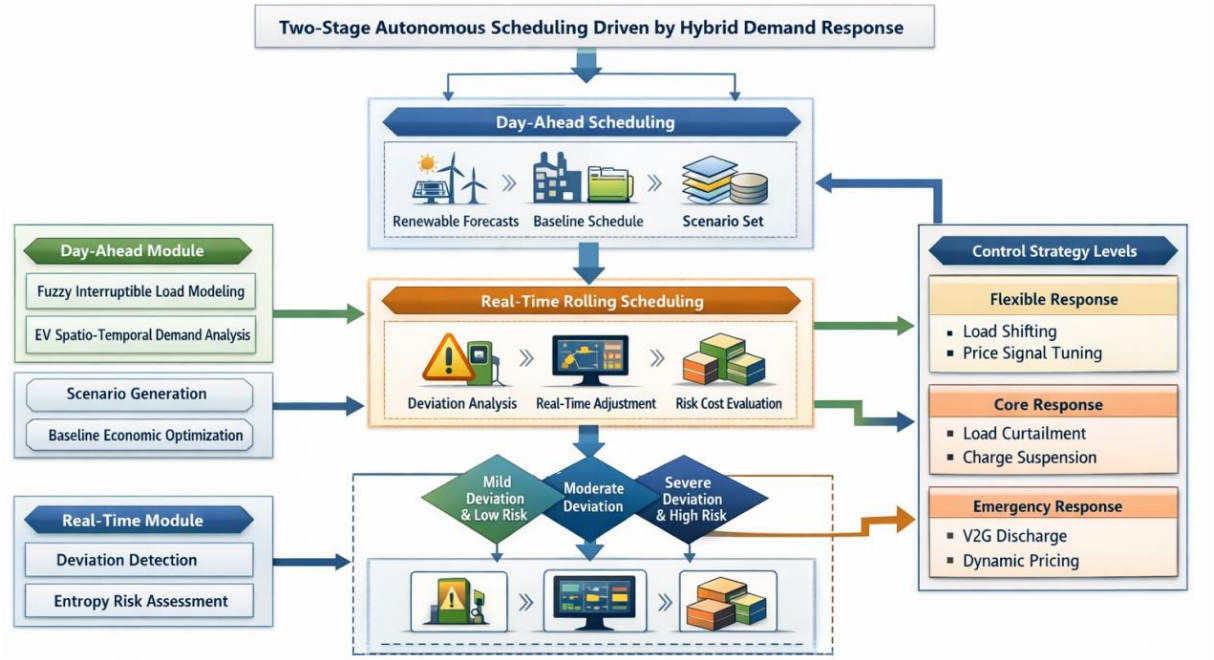

Figure 2: Two-phase autonomous scheduling process driven by hybrid demand response

(1) Economic dispatch modeling in day-ahead stage

The day-ahead phase mainly generates the benchmark power allocation scheme for the future scheduling cycle, and its core is to integrate the fuzzy load response and random charging demand into the objective function. Let the scheduling time domain be t=1,2,⋯,T, then the comprehensive cost function of the day-ahead phase can be expressed as follows.

$$\min F^{DA} = \sum_{t=1}^{T} \left(c_t^g P_t^g + c_t^{es} |P_t^{es}| + c_t^{il} \mathbb{E}(\tilde{L}_t^{dr}) + c_t^{ev} P_t^{ev} \right) \tag{5}$$

where, P_t^g is the power exchanged with the main network, P_t^{es} is the charging and discharging power of energy storage, $\mathbb{E}(\tilde{L}_t^{dr})$ is the fuzzy expected response of interrable load, and P_t^{ev} is the aggregated charging power of EV. Here, the fuzzy expectation is used to convert the response boundary under the action of temperature, electricity price and user willingness into a computable quantity, which is used to alleviate the defect that the static load model is difficult to describe the time-varying characteristics. At the same time, the system also needs to meet the power balance constraint:

$$P_t^{pv} + P_t^{wt} + P_t^g + P_t^{es} = L_t^b + P_t^{ev} - \mathbb{E}(\tilde{L}_t^{dr}) \tag{6}$$

As well as constraints such as device capacity, energy storage state of charge and user behavior boundaries. This stage essentially generates an economic operating benchmark that provides a reference boundary for intraday corrections.

(2) Spatio-temporal behavior coupling and scene generation of electric vehicles

Due to the obvious spatio-temporal heterogeneity of the arrival time, length of stay and SOC of evs in the park, this paper synchronously introduces the charging demand prediction module in the day-ahead stage. Let the charging demand probability of the KTH region at time t be pk,t, then it can be written as follows.

$$p_{k,t} = \frac{\exp\left(\theta_1 S_{k,t} + \theta_2 \lambda_t + \theta_3 H_{k,t}\right)}{\sum_{j=1}^{K} \exp\left(\theta_1 S_{j,t} + \theta_2 \lambda_t + \theta_3 H_{j,t}\right)} \tag{7}$$

Here, $S_{k,t}$ represents the SOC influence term, λ_t is the dynamic electricity price, and $H_{k,t}$ is the spatio-temporal hotspot weight. This expression combines the state of charge, price stimulus and spatial aggregation degree into the probability calculation at the same time, which is used to describe the coupling relationship between user travel chain and charging decision. In order to enhance the adaptability of the benchmark scheduling to uncertain scenarios, we further construct the day-ahead scenario set Ω based on the typical scenario generation and reduction strategy, so that the scenery output fluctuation, load elasticity deviation and charge transfer demand are characterized in advance at the day-ahead stage.

(3) Rolling robust correction of intraday phase

When the system enters real-time operation, the original benchmark schedule may fail due to new energy prediction error, user-side deviation or centralized charging impact, so it needs to be dynamically corrected in the rolling time domain. Let the power deviation at time t be as follows.

$$\Delta P_t = \left(L_t^b + P_t^{ev}\right) - \left(P_t^{pu} + P_t^{wt} + P_t^{es} + P_t^{g} + P_t^{dr}\right) \tag{8}$$

Then the correction target for the intra-day phase can be written as follows.

$$\min F^{RT} = \sum_{t=1}^{T_r} \left(\lambda_1 |\Delta P_t| + \lambda_2 R_t + \lambda_3 U_t\right) \tag{9}$$

Here, R_t is the mixed entropy risk term and U_t is the regulation cost. Considering the aggregate impact of multi-source uncertainty in different scenarios, this paper defines the hybrid entropy risk as follows.

$$R_t = -\sum_{s \in \Omega_t} \pi_s \ln \pi_s + \eta \mathrm{Var}\left(\Delta P_t^{(s)}\right) \tag{10}$$

The former term characterizes the dispersion degree of scene distribution, while the latter term reflects the power deviation fluctuation intensity. Intra-day correction not only pursues instantaneous deviation reduction, but also takes into account risk controllability and subsequent scheduling stability. The rolling optimization window is solved again after each state update, which makes the method have better online adaptability.

(4) Three-level response triggering and autonomous execution mechanism

In order to avoid the conflict between rigid regulation and flexible regulation under a single trigger threshold, this paper sets up a hierarchical response mechanism in the intra-day stage. According to the power deviation and risk level, the system switches between three types of modes: elastic adjustment, core control and emergency correction. The triggering criterion can be expressed as follows.

$$\Gamma_t = \begin{cases} \text{Flexible}, & |\Delta P_t| \le \delta_1 \\ \text{Core}, & \delta_1 < |\Delta P_t| \le \delta_2 \\ \text{Emergency}, & |\Delta P_t| > \delta_2 \end{cases} \tag{11}$$

Here,δ_1,δ_2 are the dynamic update thresholds. The elastic level mainly achieves low-cost control through flexible expectation adjustment and spatio-temporal weight correction. The core stage focuses on fast voltage drop load and freezing unnecessary charging behavior. In the emergency level, vehicle discharge, dynamic compensation pricing, and cross-agent collaborative support are introduced to cope with the deep power gap. The three-level response mode is shown in Table 2. This mechanism makes the two-phase scheduling method no longer stay in the linear framework of "plan first, fix later", but form an autonomous closed loop that can be sensed, switched and fed back in real-time operation.

Table 2: Three-level response mode and autonomous execution content

Response Level	Trigger Basis	Main Control Actions	Scheduling Objective
Elastic Response	Mild power deviation and low-risk disturbance	Fine adjustment of flexible loads, EV charging time shifting, correction of price signals	Reduce cost and maintain economical operation
Core Response	Moderate deviation and local limit-violation risk	Rapid load shedding, charging freeze, strong energy storage support	Quickly suppress fluctuations and stabilize key nodes
Emergency Response	Large deviation and persistent high-risk state	V2G discharging, dynamic compensation pricing, cross-agent collaborative reconfiguration	Prevent instability and ensure power supply security

In summary, on the one hand, our proposed two-stage autonomous scheduling method improves the adaptation of the benchmark scheme by absorbing the fuzzy expectation of interrisible load and the spatio-temporal collaboration results of electric vehicles in the day-ahead phase. On the other hand, in the intra-day stage, the rolling robust correction and three-level response mechanism are used to enhance the rapid processing ability of sudden disturbances and multi-source uncertainties. Combined with the multi-agent cooperative scheduling architecture constructed in 3.1, this method can provide a unified method basis for multi-scenario simulation, response efficiency evaluation and robustness analysis in subsequent experiments.

4 Data acquisition and model parameter setting

4.1 Multi-source data and typical scene construction of microgrid in industrial parks

In order to ensure that the autonomous scheduling model of hybrid demand response can reflect the coupling characteristics of source-side fluctuations, load-side response and vehicle-network interaction in the microgrid of industrial parks at the same time, we construct the simulation data set in a multi-source data-driven way. The data mainly consists of four parts: historical load data of the park, distributed new energy output data, electric vehicle charging behavior data, and meteorological and price data. Among them, the historical load data is used to describe the change law of base load and interrusible load in different production periods. The new energy output data is used to depict the random fluctuations of photovoltaic and wind power under different weather conditions. The electric vehicle charging data is used to identify the time distribution, spatial migration of charging demand and the difference of state of charge.

Meteorological and price data are used to reflect the impact of temperature changes and electricity price incentives on user response boundaries.

In terms of specific data configuration, this paper takes 365 days of continuous campus operation data as the basic sample, and uses 15 min as the scheduling time resolution, so that each type of time series data forms 35040 sampling points in total. The base load data covers three types of park production load, office load and public service load. The peak value of base load is set to 4.8MW, and the valley value is set to 2.1MW. The rated capacity of interruptable load is set to 1.2 MW, which accounts for 25.0% of the peak load of the park. The new energy side includes 2.5 MW PV system and 1.8 MW wind power unit, the rated power of the energy storage system is set to 1.5 MW, and the rated capacity is 3.0 MWh. A total of 300 access vehicles are set up in the electric vehicle part, corresponding to three types of production and transportation vehicles, commuting vehicles and external service vehicles, and the average daily charging demand in the benchmark scenario is about 2.4 MWh. In order to improve the consistency of multi-source data, this paper performs missing value imputation, outlier elimination and unified timestamp alignment on the original samples, and then extracts key features such as temperature, electricity price, charging start and end time, length of stay, state of charge, wind power output and energy storage state of charge respectively to form a heterogeneous database that can be used for two-stage autonomous scheduling.

The multi-source data composition and its numerical configuration of the microgrid in industrial parks are shown in Table 3.

Table 3: Multi-source data composition and numerical configuration

Data Category	Main Content	Numerical Configuration	Role in the Model
Historical Load Data	Base load, interruptible load, peak-valley curve	365 days, 15 min interval, 35,040 points; peak value 4.8 MW, valley value 2.1 MW	Describes time-varying load patterns and supports demand response modeling
Renewable Generation Data	Photovoltaic output, wind power output	PV 2.5 MW, wind power 1.8 MW	Characterizes source-side fluctuations and supports power balance analysis
Energy Storage Operation Data	Charging/discharging power, state of charge	Rated power 1.5 MW, capacity 3.0 MWh	Supports intraday correction and reserve regulation
EV Charging Data	Charging period, charging amount, dwell time, regional distribution	300 vehicles, average daily charging demand 2.4 MWh	Identifies charging hotspot migration and supports spatiotemporal behavior prediction
Meteorological and Price Data	Temperature, solar irradiance, wind speed, time-of-use electricity price	Synchronously sampled with load data, 35,040 points	Supports temperature sensitivity analysis and price response modeling

In terms of typical scenario construction, this paper sets up four types of representative operation scenarios to test the adaptability of the model under different uncertainty intensities and system states. Scenario A is a normal operation scenario with mild temperature fluctuation ±3 ℃, benchmark electricity price and 20% EV penetration. Scenario B is a high uncertainty

scenario, where EV penetration rates of ±8 ℃ extreme temperature fluctuations and ±30% and 40% drastic electricity price changes are set. Scenario C is a high elastic demand scenario with continuous high temperature +10 ℃, low electricity price incentive and 50% EV penetration. Scenario D is a deep energy deficit scenario, with PV output plunging by 60%, rigid load spiking, and EV availability below 30%.

In order to facilitate the subsequent comparison of the differences of different autonomous scheduling strategies in terms of adjustment cost, power recovery time, risk entropy and renewable energy consumption rate, this paper further uses Monte Carlo method to conduct extended sampling for four types of typical scenarios, and generates 100 groups of random operating samples for each type of scenario, forming a total of 400 groups of scenario instances. The subsequent parameter sensitivity analysis will focus on the range of adjustment factor γ value 0.05-0.15 and electricity price elasticity coefficient β value 0.1-0.2, so as to evaluate the robustness and adaptability of the model under the condition of key parameter fluctuation.

4.2 Autonomous scheduling model parameters and experimental scheme Settings

After completing the multi-source data sorting and the construction of typical scenarios, the key parameters and experimental process of the autonomous scheduling model are uniformly set. In order to balance the calculation accuracy and real-time correction efficiency, the simulation platform was built by MATLAB. The optimization time domain of the day-ahead stage was set as 24 hours, the rolling correction window was set as 1 hour, and the scheduling interval was unified as 15 minutes. Considering that the two-stage scheduling includes not only the interrusible load dynamic fuzzy response, but also the charging behavior migration and hierarchical response triggering of electric vehicles, the genetic optimization module is introduced in the solution process, where the population size is set to 50, the maximum iteration number is set to 100, the crossover probability is set to 0.7, and the mutation probability is set to 0.1 to balance the global search ability and the solution speed.

The comprehensive objective function is composed of three parts: operation cost, power deviation and risk penalty, and the weights are 0.4, 0.3 and 0.3 respectively, so that the model takes into account the balance between supply and demand and operation safety while ensuring economy. Aiming at the uncertainty of the demand response side, this paper further controls the adjustment factor between 0.05 and 0.15, and the electricity price elasticity coefficient between 0.10 and 0.20 for the subsequent sensitivity analysis and robustness test. The experimental scheme is divided into three levels: firstly, the feasibility of interrustable load modeling, spatio-temporal prediction of electric vehicles, and two-stage scheduling process are verified. Then, the differences of different strategies in regulation cost, power recovery time, renewable energy consumption rate, and risk level are compared under four typical scenarios.

5 Evaluation of autonomous scheduling model for microgrid in industrial parks

5.1 Basic performance evaluation of autonomous scheduling model

In order to verify whether the built autonomous scheduling model has stable and reliable basic capabilities before entering the multi-scenario efficiency analysis, we conduct evaluation according to the three levels of "load modeling accuracy - charging behavior prediction ability - comprehensive identification performance". The evaluation content is consistent with the model design above, focusing on the adaptability of the dynamic fuzzy modeling of

interruptable load under temperature disturbance, the prediction accuracy of the coupled spatio-temporal behavior modeling of electric vehicle charging, and the overall performance of the two-stage autonomous scheduling framework in terms of basic discriminant indicators. This arrangement can first determine whether the model "predicts correctly and identifies stably", and then further analyze its adjustment effect in complex working conditions.

(1) Error analysis of dynamic fuzzy modeling for interruptible load

Figure 3 shows the comparison of the error of dynamic fuzzy modeling for interrable load. In the figure, the proposed method is compared with the static threshold model and the triangular fuzzy model, and the mean absolute percentage error under the four working conditions of mild fluctuation, heating disturbance, high temperature disturbance and extreme fluctuation is investigated respectively.

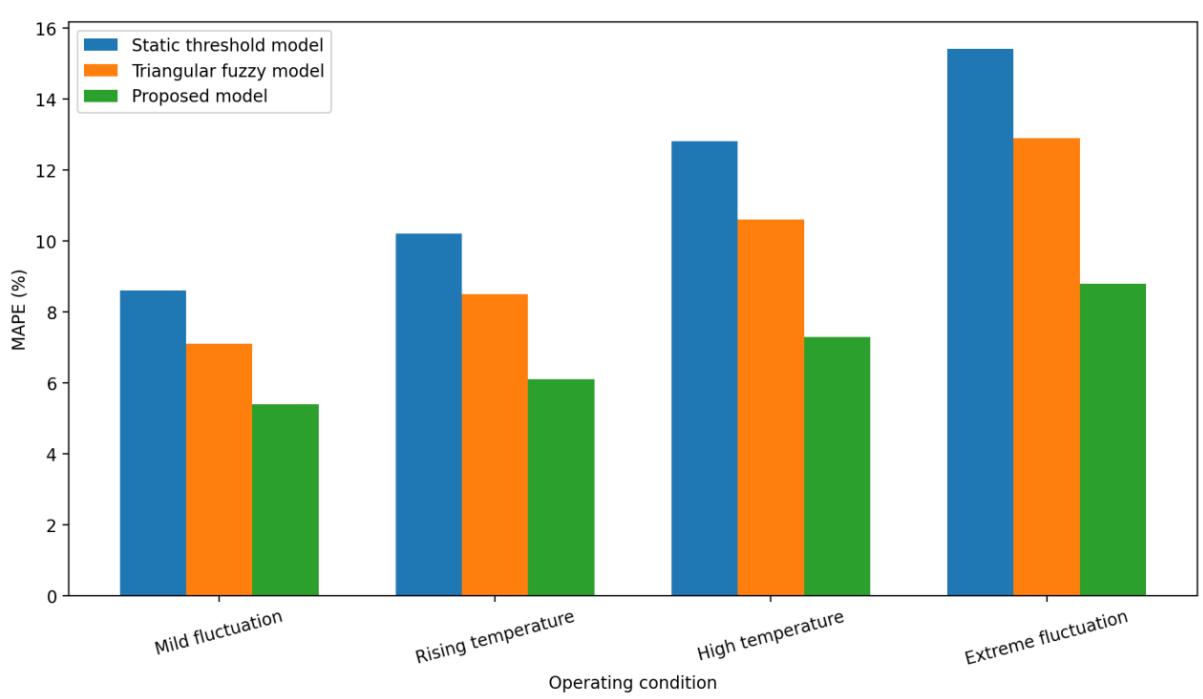

Figure 3: Comparison plot of error in dynamic fuzzy modeling of interruptible load

Figure 3 shows that the error of the proposed model is always lower than the other two comparison methods under the four types of working conditions, and the advantage is more obvious as the disturbance is enhanced. Under extreme fluctuation conditions, the error of the static threshold model rises to 15.4%, the triangular fuzzy model is 12.9%, and the proposed model is controlled at 8.8%. This shows that when temperature, electricity price and user willingness change together, the fixed boundary or single fuzzy expression is difficult to describe the load response interval stably. After introducing dynamic trapezoidal fuzzy boundary and adaptive membership adjustment, the model has stronger adaptation ability to high fluctuation conditions. Further calculation shows that the average error of the proposed model under four types of working conditions is 6.9%, which is 4.9 percentage points lower than that of the static threshold model (11.8%) and 2.9 percentage points lower than that of the triangular fuzzy model (9.8%). It can be seen that the proposed method has formed a more stable fundamental representation capability on the interruptible load side, which provides a more credible demand response input for the subsequent scheduling solution.

(2) Analysis of electric vehicle charging hotspot prediction effect

Figure 4 shows the performance of EV charging hotspot prediction. In the figure, four

typical functional areas including production area, office area, logistics area and service area are selected to compare the hot spot matching rate of the static probability model, the traditional Markov model and the proposed method.

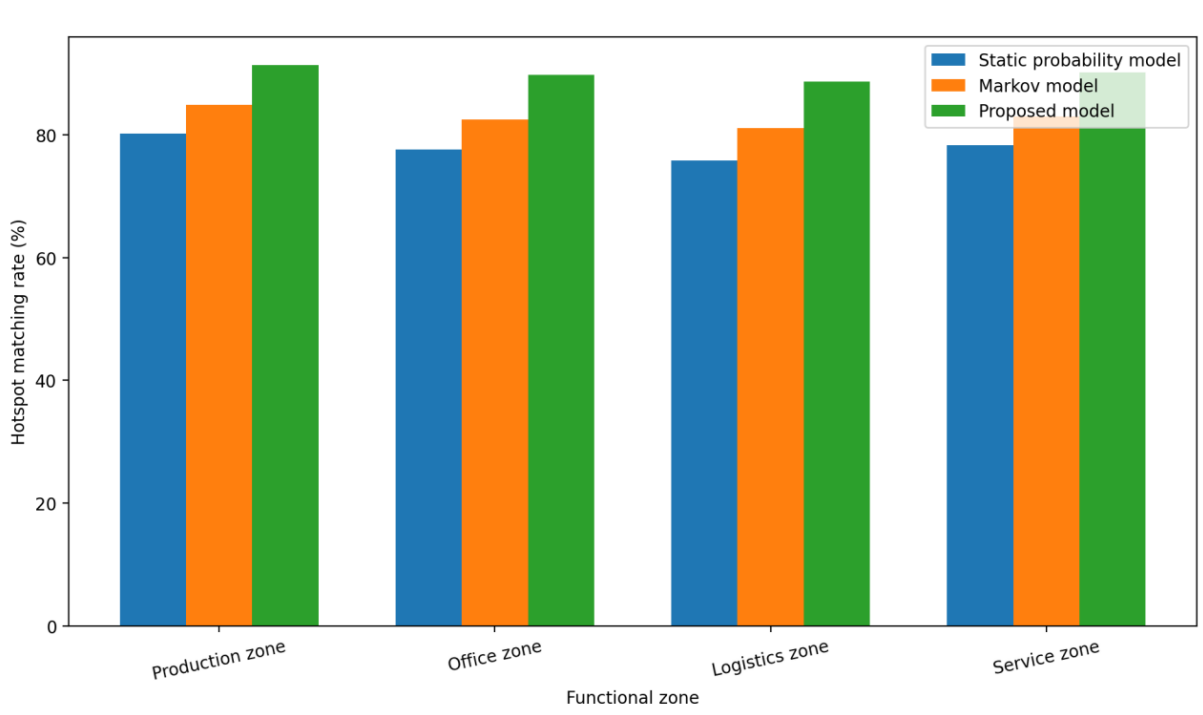

Figure 4: Comparison plot of EV charging hotspot prediction performance

Figure 4 shows that the proposed method achieves higher hot spot matching rates in all four types of regions. Production area, office area, logistics area and service area reached 91.4%, 89.8%, 88.7% and 90.2%, respectively, with an average of 90.0%. In contrast, the average matching rate is 82.9% for the traditional Markov model and only 78.0% for the static probabilistic model. Especially in the areas with more frequent demand migration and more scattered arrival time, such as logistics area and office area, the matching rates of the proposed method still maintain 88.7% and 89.8% respectively, indicating that the proposed method has a better ability to describe the behavior migration under spatio-temporal heterogeneity and price induced. This is in good agreement with the Gaussian mixture distribution, non-homogeneous Markov chain and state-dependent charging probability model constructed in the previous section. In summary, the hotspot recognition accuracy of the proposed method is 12.0 and 7.1 percentage points higher than that of the static probability model and the traditional Markov model, respectively, indicating that the proposed method can more accurately capture the dynamic transfer trend of electric vehicle charging demand in the park.

(3) Comprehensive basic performance evaluation of autonomous scheduling model

After the verification of load modeling and charging behavior prediction, this paper further evaluates the basic performance of the autonomous scheduling model from the perspective of comprehensive identification, and the results are shown in Table IV.

Table 4: Comparison of basic performance evaluation results

Method	Accuracy/%	Precision/%	Recall/%	F1/%	MAPE/%	RMSE
Traditional Single-Level Response Model	84.6	83.9	82.7	83.3	10.8	0.286
Static Hybrid Demand Response Model	88.1	87.4	86.8	87.1	8.4	0.221
Proposed Model	93.7	92.9	92.1	92.5	5.9	0.148

Table 4 shows that the proposed model maintains above 92% in terms of Accuracy, Precision, Recall and F1, where Accuracy reaches 93.7% and F1 reaches 92.5%, which are 9.1 and 9.2 percentage points higher than those of the traditional single-stage response model respectively. Compared with the static hybrid demand response model, it increases by 5.6 and 5.4 percentage points. At the same time, the MAPE of the proposed model is reduced to 5.9% and RMSE is reduced to 0.148, indicating that the model is not only more stable at the classification and recognition level, but also shows higher accuracy at the continuous value fitting level. The key reasons for this result are as follows: on the one hand, the dynamic fuzzy modeling of interruptable load reduces the response deviation caused by the static boundary; On the other hand, the spatio-temporal behavior coupling prediction of electric vehicles improves the prior recognition ability of aggregated charging demand. In addition, the two-phase autonomous scheduling framework organizes the information flow and control flow in a unified way, which makes the model have better stability and interpretability at the basic level. On the whole, our proposed model performs best among the three comparison methods, with the overall improvement of the basic performance index of 5.4%-9.2%and the error index of about 29.8%-45.4%decrease, which lays a more reliable model foundation for the effectiveness evaluation of the following four typical scenarios.

It can be seen from the results of 5.1 that the autonomous scheduling model constructed in this paper shows stable basic capabilities on the input side, prediction side and discrimination side: the average error of load modeling is controlled at 6.9%, the average matching rate of electric vehicle hotspots reaches 90.0%, and the comprehensive Accuracy and F1 reach 93.7% and 92.5% respectively. This shows that the model can well support the subsequent adjustment cost analysis, power recovery process comparison and three-level response mechanism efficiency evaluation in multiple scenarios.

5.2 Efficiency evaluation of autonomous scheduling for hybrid demand response

After the basic performance verification, this paper further analyzes the actual efficiency of the hybrid demand response autonomous scheduling method from the system operation level. The evaluation focuses on the comprehensive adjustment cost, the power deviation recovery process and the triggering effect of the three-level response mechanism in four typical scenarios, to test the adaptability of the model under the conditions of normal operation, high uncertainty, high elastic demand and deep energy shortage. The evaluation indicators mainly include comprehensive regulation cost, power recovery time, renewable energy consumption rate and response trigger frequency, which can completely reflect the operation quality and regulation level of the microgrid in industrial parks under complex disturbances.

(1) Comprehensive adjustment cost analysis under four typical scenarios

Figure 5 shows the comparison of comprehensive regulation costs under four typical scenarios. The figure compares the comprehensive regulation cost of the traditional single-stage response strategy, the static hybrid demand response strategy and the proposed method in four

types of operation scenarios.

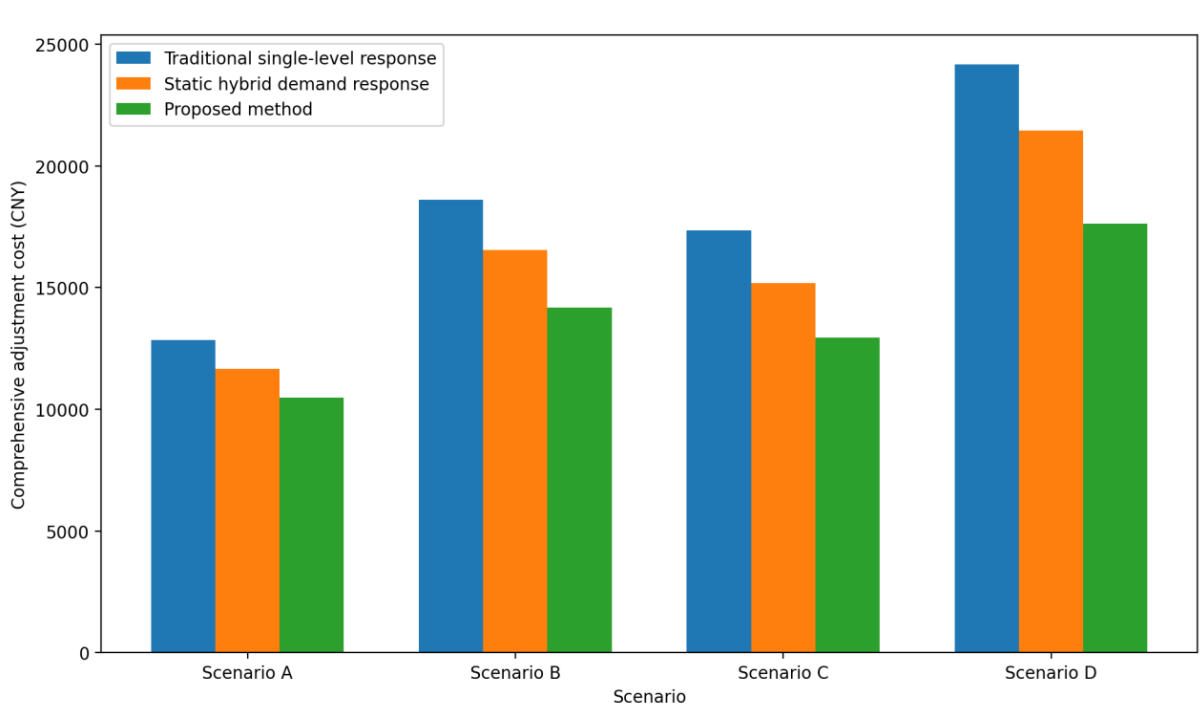

Figure 5: Comprehensive Adjustment Cost under Four Typical Scenarios

It can be seen from Figure 5 that the regulation cost of the three methods in the four types of scenarios increases with the upgrading of disturbance intensity, but the proposed method always maintains the lowest level. In scenario A, the comprehensive adjustment costs of the traditional single-stage response strategy, the static hybrid demand response strategy and the proposed method are 12840 yuan, 11670 yuan and 10490 Yuan, respectively. In scenario B, 18620 yuan, 16540 yuan and 14180 yuan respectively; In scenario C, they are 17350 yuan, 15180 yuan and 12960 yuan respectively; In scenario D, it is further increased to 24,180 yuan, 21,460 yuan and 17,630 yuan. It can be seen that in the deep energy shortage scenario, the cost advantage of the proposed method is the most obvious, which is reduced by 6550 yuan (27.1%) compared with the traditional single-stage response strategy, and is also reduced by 17.8% compared with the static hybrid demand response strategy. This shows that when the new energy output drops sharply, the rigid load rises and the availability of electric vehicles decreases simultaneously, the two-stage autonomous scheduling can allocate the energy storage support, load adjustment and charge transfer tasks more effectively, thereby restraining the rapid amplification of additional regulation costs. Overall, the average adjustment cost of the proposed method under the four types of scenarios is 13815 yuan, which is 24.3% lower than that of the traditional strategy of 18247.5 yuan, showing better economy.

(2) Analysis of power deviation recovery process

The power deviation recovery process under different strategies is shown in Figure 6. Figure 6 selects the most representative set of disturbance processes in the deep energy deficit scenario to compare the deviation recovery trajectories of the three strategies.

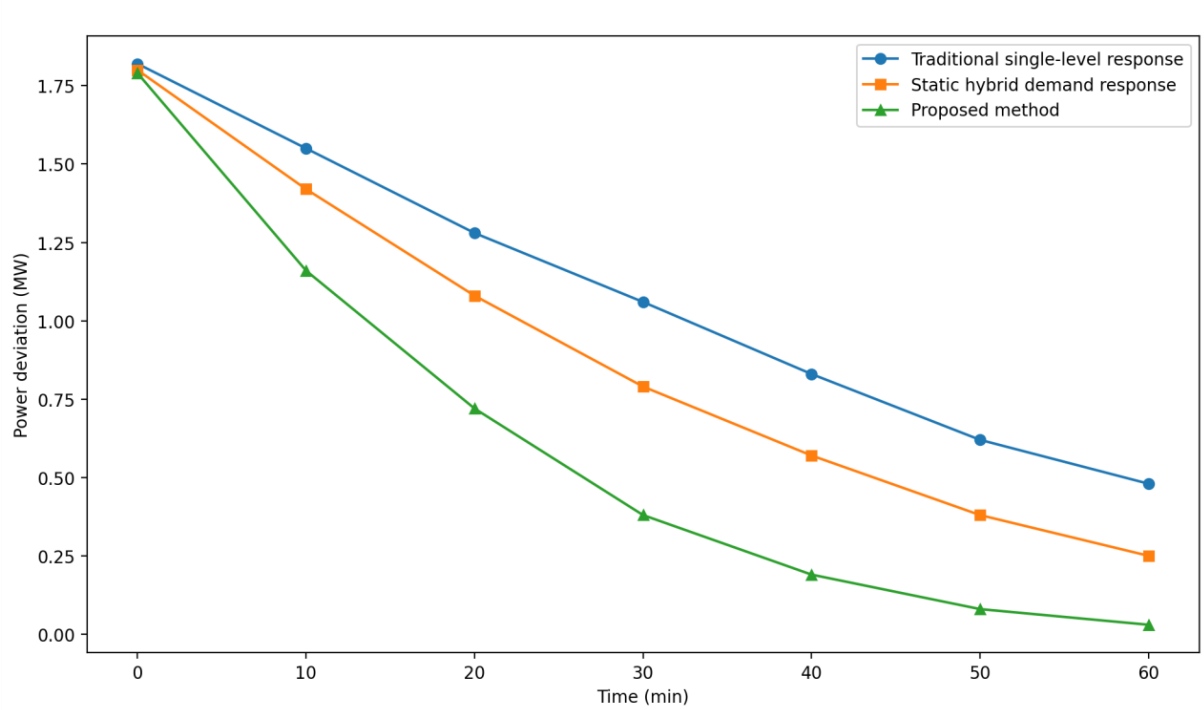

Figure 6: Power Deviation Recovery in Scenario D

It can be seen from Figure 6 that although the traditional single-stage response strategy can gradually reduce the power gap after the disturbance occurs, the recovery process is obviously lagging behind, and the deviation is still 0.48MW after 60 min. The decline speed of the static hybrid demand response strategy is improved, but there is still a deviation of 0.38 MW at 50 min. In contrast, the proposed method has reduced the deviation from 1.79 MW voltage to 1.16 MW at 10 min, further reduced it to 0.38 MW at 30 min, controlled it to 0.19 MW at 40 min, and only 0.03 MW remained at 60 min. It shows that the proposed method can quickly complete the chain closed loop from state identification, risk assessment to response execution, especially under high impact conditions, it has a stronger ability to plan energy storage, interrable load and aggregated response of electric vehicles. If the power deviation drops below 0.20 MW as the recovery criterion, the recovery time of the proposed method is about 40 minutes, while the static hybrid demand response strategy and the traditional single-stage response strategy need more than 50 minutes and 60 minutes respectively, and the recovery efficiency advantage is more obvious. In general, the proposed method can shorten the deviation recovery time by about 20 min compared with the traditional single-stage response strategy in the deep energy shortage scenario, and shorten the deviation recovery time by about 10 min compared with the static mixed demand response strategy, indicating that it has stronger short-term fluctuation suppression ability and collaborative adjustment efficiency under high impact conditions.

(3) Analysis of the triggering effect of the three-level response mechanism

The three-level response trigger frequency is shown in Figure 7. This figure counts the trigger times of elastic response, core response and emergency response in four types of scenarios, which is used to analyze the effect distribution of the hierarchical regulation mechanism in different operating states.

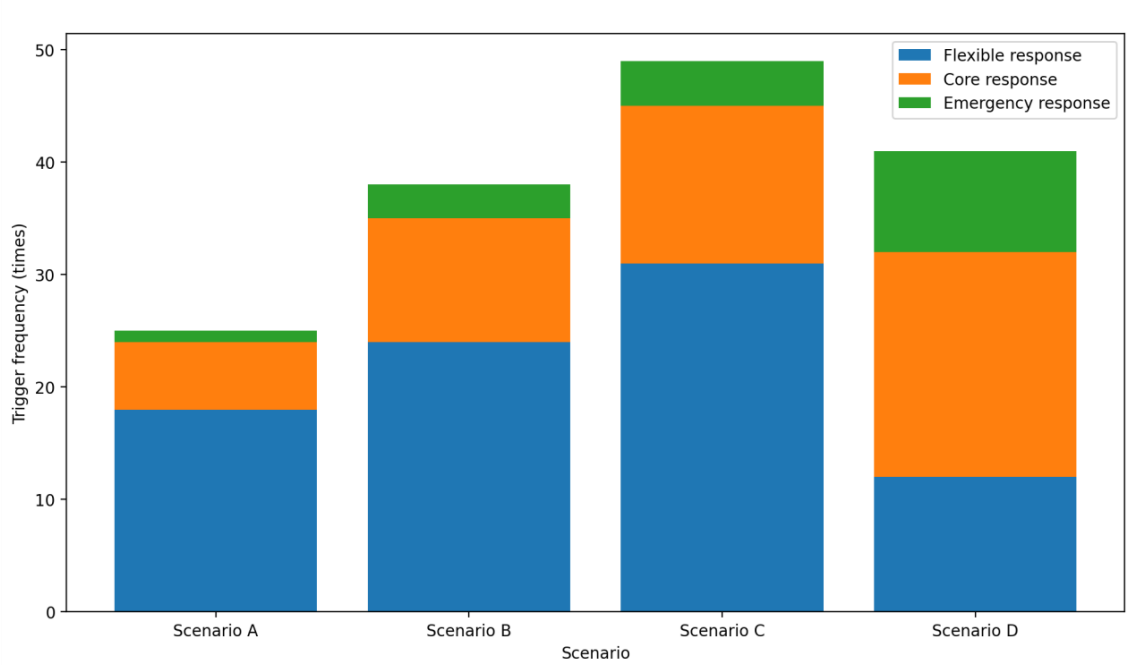

Figure 7: Trigger Frequency of Three-Level Response

As can be seen from Figure 7, in scenario A, the system is dominated by elastic response, triggering 18 times, core response 6 times, and emergency response only 1 time, indicating that the balance can be maintained mainly by load fine-tuning and price signal correction under normal operation. After entering scenario B, the elastic response increased to 24 times, the core response increased to 11 times, and the emergency response increased to 3 times, indicating that more intermediate level control intervention was needed in the high uncertainty scenario. In scenario C, the three types of responses reached 31, 14 and 4, respectively, indicating that flexible resources were invoked more frequently under the condition of high elastic demand. In scenario D, the elastic response drops to 12 times, while the core response and emergency response rise to 20 times and 9 times, indicating that in the deep energy shortage scenario, the system must rely more on strong intervention methods such as rigid load voltage drop, charge freezing and vehicle discharge. It can be seen that the three-level response mechanism can automatically allocate regulation resources according to the disturbance intensity, making the control focus clearer in different scenarios. In summary, Scenario A and Scenario C are dominated by elastic response, and scenario D is dominated by core response and emergency response. The three-level mechanism successfully realizes a smooth switch from normal economic operation to extreme risk disposal.

(4) Comprehensive comparison of key operating indicators

To further demonstrate the comprehensive regulation effect of the proposed method, the key operating indicators under four types of typical scenarios are shown in Table 5.

Table 5: Comparison of key operating indicators under four types of typical scenarios

Method	Accuracy/%	Precision/%	Recall/%	F1/%	MAPE/%	RMSE
Traditional Single-Level Response Model	84.6	83.9	82.7	83.3	10.8	0.286
Static Hybrid Demand Response Model	88.1	87.4	86.8	87.1	8.4	0.221
Proposed Model	93.7	92.9	92.1	92.5	5.9	0.148

Table 5 shows that the proposed method maintains a good comprehensive performance in all four types of scenarios. Among them, the renewable energy consumption rate of scenario C reaches 86.8%, which is the highest among the four scenarios, indicating that under the condition of high elastic demand, demand-side resources are easier to form synergy with new energy fluctuations. Although scenario D is greatly affected by extreme disturbances, the proposed method still controls the comprehensive adjustment cost at 17,630 yuan and the recovery time within 40 min, showing a strong risk tolerance ability. Considering all the scenarios, the average renewable energy consumption rate of the proposed method reaches 80.3%, and the average recovery time is 32 min. Compared with the traditional strategy, the proposed method shows better adjustment effect in economy, response speed and new energy utilization level. Therefore, the autonomous scheduling of hybrid demand response can not only reduce the normal operation cost, but also maintain good adjustment resilience in high fluctuation and high-risk scenarios, which provides effective support for the stable operation of microgrid in industrial parks.

5.3 Discussion

From the above results, it can be seen that the hybrid demand response autonomous scheduling model constructed by us shows good stability in both basic recognition performance and scene operation efficiency, which indicates that it is effective to incorporate the multi-agent cooperation mechanism, the dynamic fuzzy modeling of interrusible load, the spatio-temporal behavior prediction of electric vehicles, and the two-stage scheduling method into the unified framework. Although the implementation process of traditional single-stage response strategy is relatively straightforward, it has limited ability to distinguish the source of disturbance and can only be passively corrected after the deviation has been amplified. Therefore, it is prone to slow recovery speed and high adjustment cost in high uncertainty and deep energy deficit scenarios. The static hybrid demand response method has been improved over the traditional strategy, but its parameter boundary and trigger logic are relatively fixed. When temperature, electricity price, load and charging behavior change simultaneously, it is still difficult to accurately reflect the real adjustable space of demand side resources.

The key reason why the proposed method can achieve better results in terms of comprehensive regulation cost, power recovery time and renewable energy consumption rate is that it does not regard all kinds of regulation objects in the park microgrid as independent units, but integrates the local decision-making of source, storage, load and vehicle into the unified scheduling chain through multi-agent cooperation. Then, the continuous response to perturbations of different time scales is realized by the connection mechanism of day-ahead benchmark optimization and intra-day rolling correction. Especially, the introduction of the three-level response mechanism enables the system to automatically switch the regulation mode according to the deviation intensity, avoiding the problem of too strong control in slight fluctuations and insufficient regulation in severe disturbances.

Of course, there is still room for further improvement of the research in this paper. The current experiments are mainly based on simulation scenarios, which can better reflect the typical operation characteristics of the park microgrid, but the response effects under more complex market environments, multi-park collaborative scenarios and communication delay conditions still need to be verified. In the future, online learning and dynamic parameter update mechanism can be introduced on a platform closer to real operation to further improve the generalization ability and engineering applicability of the model.

6 Conclusions

Focusing on the problem of supply-demand imbalance in the microgrid of industrial parks with a high proportion of new energy access, this paper constructs an autonomous scheduling model of hybrid demand response with multi-agent cooperation, and forms a two-stage method of "day-ahead optimization-intra-day modify-three-level response execution". The research shows that the dynamic fuzzy modeling improves the ability to describe the interlacable load response boundary, the spatio-temporal and behavioral coupling prediction of electric vehicles improves the accuracy of hot spot recognition, and the multi-agent cooperation and hierarchical trigger mechanism enhance the rapid adjustment ability under complex disturbances. In the experiment, the model Accuracy reaches 93.7%, F1 reaches 92.5%, the average adjustment cost is reduced to 13,815 yuan, the renewable energy consumption rate of scenario C reaches 86.8%, and the power recovery time of scenario D is controlled within 40 minutes. In general, the method of this paper takes into account both economic operation and risk suppression, which provides technical support for the microgrid of industrial parks to move from one-way control to autonomous collaboration. In the future, further extended research can be carried out for real park platforms and online learning scenarios.

Funding

This work was supported by Chongqing Municipal Commission of Education Science and Technology Research Program Project: Research on Power Dispatch of Industrial Park Microgrid Considering Uncertainty of Hybrid Demand Response (KJQN202504202).

References

[1] China Energy Research Society. China Energy Big Data Report (2024)[J]. China Energy Research Society, 2024, 6(26). DOI:10.13334/j.1003-0417.power.2024.06.001.

[2] Li J F, Wang Y, Cheng X X, Xiong X Z, Sun J K. Capacity Allocation Method of Photovoltaic-Storage in Microgrid System Based on Bi-level Optimization[J]. Distributed Energy, 2024, 9(1): 80-88. DOI:10.19905/j.cnki.deny.2024.01.010.

[3] Situ Y, Zhou L D, Chen F C, et al. Research on Multi-objective Configuration Optimization of Multi-energy Microgrid in Intelligent Park Based on Typical Scenario Set[J]. Acta Energiae Solaris Sinica, 2022, 43(9): 515-526. DOI:10.19912/j.0254-0096.tynxb.2021-0778.

[4] El Mezdi K, El Magri A, Bahatti L. Advanced control and energy management algorithm for a multi-source microgrid incorporating renewable energy and electric vehicle integration[J]. Results in Engineering, 2024, 23: 102642. DOI:10.1016/ j.rineng.2024.102642.

[5] Wang F, Li M Y, Zhang X D, et al. Demand Response Resource Potential Assessment Method, Application and Prospect[J]. Automation of Electric Power Systems, 2023, 47(21): 173-191. DOI:10.7500/AEPS20230227005.

[6] Kong X Y, Liu C, Chen S S, et al. Multi-time Node Response Potential Assessment Method of Adjustable Resource Cluster Considering Dynamic Process[J]. Automation of

Electric Power Systems, 2022, 46(18): 55-64. DOI:10.7500/AEPS20210906007.

[7] Fan S, Wei Y H, He G Y, et al. Discussion on Demand Response Mechanism for New Power System[J]. Automation of Electric Power Systems, 2022, 46(7): 1-12. DOI:10.7500/AEPS20211014006.

[8] Li J, Yang M, Zhang Y, Li J, Lu J. Micro-grid day-ahead stochastic optimal dispatch considering multiple demand response and electric vehicles[J]. Energies, 2023, 16: 3356. DOI:10.3390/en16083356.

[9] Zhu Y Y, Wang Z J, Wang H, et al. Research on Coordinated Optimization Strategy of Hybrid Energy Storage in Microgrid Based on Hierarchical Control[J]. Acta Energiae Solaris Sinica, 2024, 42(3): 235-242. DOI:10.19912/j.0254-0096.tynxb.2022-0988.

[10] Zhao Y, Chen Y T, Sun W Y. Research on Interval Scheduling Method and Market Transaction Strategy of Multi-microgrid Distribution System[J]. Power System Technology, 2022, 46(1): 1-10. DOI:10.13335/j.1000-3673.pst.2021.1146.

[11] Ji Y, Wang J H. Online Optimal Scheduling of Microgrid Based on Deep Reinforcement Learning[J]. Control and Decision, 2021, 35(8): 1-10. DOI:10.13195/j.kzyjc.2020.0367.

[12] Yang F U, Jiang Y, Zhenkun L I, et al. Optimal Economic Dispatch for Microgrid Considering Shiftable Loads[J]. Chinese Journal of Electrical Engineering, 2022, 34(16): 2612-2622. DOI:10.13334/j.0258-8013.csee.2022.16.002.

[13] Mortaji H, Ow S H, Moghavvemi M, et al. Load Shedding and Smart-Direct Load Control Using Internet of Things in Smart Grid Demand Response Management[J]. IEEE Transactions on Industry Applications, 2023, PP(6): 1-1. DOI:10.1109/TIA. 2023.3288290.

[14] Zeng J, Wang Q, Liu J, et al. A Potential Game Approach to Distributed Operational Optimization for Microgrid Energy Management With Renewable Energy and Demand Response[J]. IEEE Transactions on Industrial Electronics, 2023, 66(6): 4479-4489. DOI:10.1109/TIE.2022.3227290.

[15] Ma D, et al. Proactive Robust Hardening of Resilient Power Distribution Systems[J]. arXiv.org, 2025, 3(6). DOI:10.48550/arXiv.2501.02123.

[16] Kumar S S, Iruthayarajan M W, Saravanan R. Hybrid technique for optimizing charging-discharging behaviour of EVs and demand response for cost-effective PV microgrid system[J]. Journal of Energy Storage, 2024, 96: 112667. DOI:10.1016/j. est.2024.112667.

[17] Ma X, Peng B, Ma X, Tian C, Yan Y. Multi-timescale optimization scheduling of regional integrated energy systems[J]. Energy, 2023, 11(15). DOI:10.1016/j.energy. 2023.128678.

[18] Shi K, Tan Z, Zhang L. Integrated Demand Response and Optimization Control Strategy in Smart Micro-Grids[J]. 2025 International Conference on Multi-Agent Systems for Collaborative Intelligence (ICMSCI), 2025: 1329-1335. DOI:10.1109/ ICMSCI62561.2025.10894524.

[19] Guanzhong G, Li Y, Yang S, et al. Research on Regional Power Grid Scheduling Strategy

With Flexible Resource Clusters Based on Multi-Agent Deep Reinforcement Learning[J]. IET Smart Grid, 2025, 8(1). DOI:10.1049/stg2.70028.

[20] Shen Y, Xu J, Wang X, et al. Collaborative hierarchical scheduling model of interconnected multi-microgrid and ADN considering DR with different strategies[J]. AIP Advances, 2024, 14(4): 13. DOI:10.1063/5.0185173.

[21] Fu X, Zeng G, Zhu X, et al. Optimal scheduling strategy of grid-connected microgrid with ladder-type carbon trading based on Stackelberg game[J]. Frontiers in Energy Research, 2022, 10(10): 961341. DOI:10.3389/fenrg.2022.961341.

[22] Hua F, Hanbing Z, Jichao Y, et al. Optimal Control Architecture of Smart Energy Interconnected System with Multi-Factor Integration in New Power System[J]. 2024 IEEE 6th International Conference on Civil Aviation Safety and Information Technology (ICCASIT), 2024: 1382-1386. DOI:10.1109/ICCASIT62299.2024. 10827993.